ELSEVIER

J. Biochem. Biophys. Methods 30 (1995) 163–177

JOURNAL OF
biochemical and
biophysical
methods

Research article

Base-pair exchange kinetics of the imino and amino protons of the 3′-phenazinium tethered DNA–RNA duplex, r($^{5'}$GAUUGAA$^{3'}$):d($^{5'}$TCAATC$^{3'}$-Pzn), and their comparison with those of B-DNA duplex

T.V. Maltseva [a], V.F. Zarytova [b], J. Chattopadhyaya [a,*]

[a] *Department of Bioorganic Chemistry, Box 581, Biomedical Center, University of Uppsala, S-751 23 Uppsala, Sweden*

[b] *Institute of Bioorganic Chemistry, Siberian Branch of Russian Academy of Sciences, Novosibirsk 630090, Russian Federation*

Received 21 October 1994; revised 9 December 1994; accepted 14 December 1994

Abstract

The dynamics of the opening-closing of the constituent base-pairs as well as of the exchange kinetics of the base-paired imino and amino protons with water in a DNA–RNA hybrid, [$^{5'}$r(G^{1}A^{2}U^{3}U^{4}G^{5}A^{6}A^7)$^{3'}$]:$^{5'}$p[d(T^{8}C^{9}A^{10}A^{11}T^{12}C^{13})]$^{3'}$-Pzn] duplex (I), are reported here in details for the first time. The exchange kinetics of amino and imino protons in the DNA–RNA hybrid (duplex I) have been compared with identical studies on the following B-DNA duplexes: d(C^{1}G^{2}T^{3}A^{4}C^{5}G^6)$_2$ (II), d[p($^{5'}$T^{1}G^{2}T^{3}T^{4}T^{5}G^{6}G^{7}C^8)$^{3'}$]:d[p($^{5'}$C^{9}C^{10}A^{11}A^{12}A^{13}C^{14}A^{15})$^{3'}$] (III), d(C^{5}G^{6}C^{7}G^{8}A^{9}A^{10}T^{11}T^{12}C^{13}G^{14}C^{15}G^{16})$_2$ (IV) and d(C^{1}G^{2}C^{3}G^{4}C^{5}G^{6}C^{7}G^{8}A^{9}A^{10}T^{11}T^{12}C^{13}G^{14}C^{15}G^{16}C^{17}G^{18}C^{19}G^{20})$_2$ (V). This comparative study shows that the life-times τ_o of various base-pairs in the DNA–RNA hybrid (I) varies in the range of ~ 1 ms, and they are quite comparable to those of the shorter B-DNA duplexes (II) and (III), but very different from the τ_o of the larger duplexes (IV) and (V): the τ_o for the base pair of T^{11} and T^{12} residues in the 20-mer (duplex V) are 2.9 ± 2.3 ms and 23.2 ± 8.9 ms, respectively, while the corresponding τ_o in the 12-mer (duplex IV) are 2.8 ± 2.2 ms and 17.4 ± 5.4 ms. It has also been shown that the total energy of activation (E_a) assessed from the exchange rates of both imino and amino protons, representing energetic contributions from both base-pair and helix opening-closing as well as from the exchange process of the imino protons from the open state with the bound water, is close to the E_a of the short B-DNA duplex ($E_a \approx 28$–47 kcal/mol).

* Corresponding author.

SSDI 0165-022X(94)00075-1

Keywords: Imino proton; Amino proton; DNA-RNA duplex; B-DNA duplex; Exchange kinetics

1. Introduction

Covalently linked agent [1], such as cholesterol [2], ethydium bromide [3], acridine [4] or phenazinium (Pzn) [5] derivative, stabilizes the DNA duplex considerably in comparison with their natural counterparts. These types of tethered oligos are potentially important in the design of antisense therapy since they are found to be relatively more resistant to the cellular nuclease as well as they are taken up quite readily through the cellular membrane compared to the natural counterpart. We showed [5] that the Pzn tethered to the 5′-end of a single stranded DNA complexes with the complementary strand with an enhancement of the thermodynamic stability of the duplex by 9–20° C compared with the natural counterparts, depending upon the number mismatches in the target DNA sequence. The Pzn mediated stabilization of the DNA duplex depends both upon the stacking ability [5] with the neighbouring nucleobases in both strands as well as on the hydration pattern in the minor and the major grooves of DNA [5]. We have also found that an otherwise unstable small DNA–RNA hybrid duplex can be stabilized [6] by using 3′-Pzn tethered DNA strand instead of natural DNA. We have thus recently reported the NMR structure [6] of 3′-Pzn tethered DNA–RNA hybrid, [$^{5'}$r($G^1A^2U^3U^4G^5A^6A^7$)$^{3'}$]:$^{5'}$p[d($T^8C^9A^{10}A^{11}T^{12}C^{13}$)]$^{3'}$Pzn] (I), which is 13° C more stable than the natural counterpart. The structure of DNA–RNA hybrid is of considerable interest because of two reasons: (i) They are formed by the reverse transcription of the viral RNA as some retroviruses such as HIV enter the infected host cells. Hence, knowledge of the global and local structure of DNA–RNA hybrid is important for the design of potential chemotherapeutic agents. (ii) Additionally, such DNA–RNA hybrids are also formed in the transcription of DNA to RNA by RNA polymerase. Hence, understanding of DNA–RNA hybrid structure in general would shed light on how the transcription machinery works at a molecular level in biology!

We here report the first detailed study on the dynamics of the exchange of imino and amino protons of a DNA–RNA hybrid, duplex (I), with water through the investigation of the opening-closing of the constituent base-pairs as well as of their exchange kinetics. These data have been subsequently compared with the identical studies with the following B-DNA duplexes: d($C^1G^2T^3A^4C^5G^6$)$_2$ (II), d[p($^{5'}T^1G^2T^3T^4T^5G^6G^7C^8$)$^{3'}$]:d[p($^{5'}C^9C^{10}A^{11}A^{12}A^{13}C^{14}A^{15}$)$^{3'}$] (III), d($C^5G^6C^7G^8A^9A^{10}T^{11}T^{12}C^{13}G^{14}C^{15}G^{16}$)$_2$ (IV) and d($C^1G^2C^3G^4C^5G^6C^7G^8A^9A^{10}T^{11}T^{12}C^{13}G^{14}C^{15}G^{16}C^{17}G^{18}C^{19}G^{20}$)$_2$ (V).

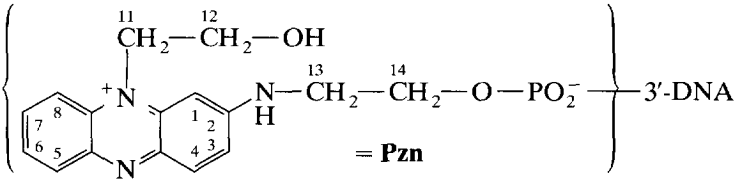

2. Materials and methods

2.1. Synthesis and sample preparation

The synthesis and preparation of 3′-Pzn tethered DNA–RNA hybrid, [$^{5'}$r($G^1A^2U^3U^4G^5A^6A^7$)$^{3'}$]:$^{5'}$p[d($T^8C^9A^{10}A^{11}T^{12}C^{13}$)]$^{3'}$Pzn] (I) and d($C^1G^2T^3A^4C^5G^6$)$_2$ (II), d[p($^{5'}T^1G^2T^3T^4T^5G^6G^7C^8$)$^{3'}$]:d[p($^{5'}C^9C^{10}A^{11}A^{12}A^{13}C^{14}A^{15}$)$^{3'}$] (III), d($C^5G^6C^7G^8A^9A^{10}T^{11}T^{12}C^{13}G^{14}C^{15}G^{16}$)$_2$ (IV) and d($C^1G^2C^3G^4C^5G^6C^7G^8A^9A^{10}T^{11}T^{12}C^{13}G^{14}C^{15}G^{16}C^{17}G^{18}C^{19}G^{20}$)$_2$ (V) have been already described [6] using an well established procedure.

2.2. Nuclear magnetic resonance spectroscopy

All ^{1}H-NMR spectra were recorded on a Bruker AMX NMR spectrometer operating at 500.13 MHz. The combination of NOESY and ROESY experiments [5] have been used to calculate the rates of exchange (k_{ex}) and life-times (τ_o) of the imino and amino protons in the duplexes (I)–(V). The mixing times used were 10, 20, 30, 40 and 60 ms. All experiments were performed at 6, 8, 10, 12, 14, 16, 18 and 20° C with 2048 complex data points in t_2, 128 complex data points in t_1. The relaxation delay between pulse sequence is 2.0 s, a sweep width of 10204.1 Hz is used in both dimensions, SL_{j4} and SL_{j5} are equal to 0.5 ms and 3 ms, respectively, the delay between spinlock pulses τ is equal to 180 ms for duplex (I) and 167 ms for duplexes (II)-(V), the carrier was set at the water frequency, 32 scans/FID were used. The correction of crosspeak volumes due to off-resonance effect has been performed using the literature procedure [5,7,8]. The influence of the spinlock pulses on the relaxation properties of water and its magnetization transfer to the exchangeable protons and on the relative intensity of the cross- and diagonal peaks, obtained after their normalizations by the diagonal peaks at $\tau_m = 0$ in the NOESY/ROESY experiments [5], has been assessed in the following manner: firstly, a blank NOESY experiment has been performed in which no spinlock pulses (i.e. reduction of water intensity by 45-τ-45 pulse sequence) [5] are included, secondly, by NOESY experiments with spinlock pulses with a recycle delay of 5 or 10 s have been performed in order to examine how the water relaxation is influenced by the delay. These control studies have shown that the difference between the relative build-up intensities of the crosspeak and diagonal intensities in the above two sets of experiments were well within the range of the experimental error ($\pm$20%). The volumes of the crosspeak to the diagonal were measured using the program AURELIA [9] with segmentation level 0.5 and 1000 iterations. The 2024 $\times$ 512 data points were resolution enhanced by a shifted squared sine-bell window function in both directions, then Fourier transformed and phase adjusted. All of the spectra were baseline-corrected in both dimensions using square polynomials. The value of the life-time τ_o has been obtained using the observable proton exchange life-time (τ_{ex}) versus inverse concentration of ammonia ([base]$^{-1}$ $< 40\ M^{-1}$) by extrapolation to the infinite concentration [10]. The accuracy in the τ_o measurement in this range of the ammonia concentration ($< 40\ M^{-1}$) is dictated

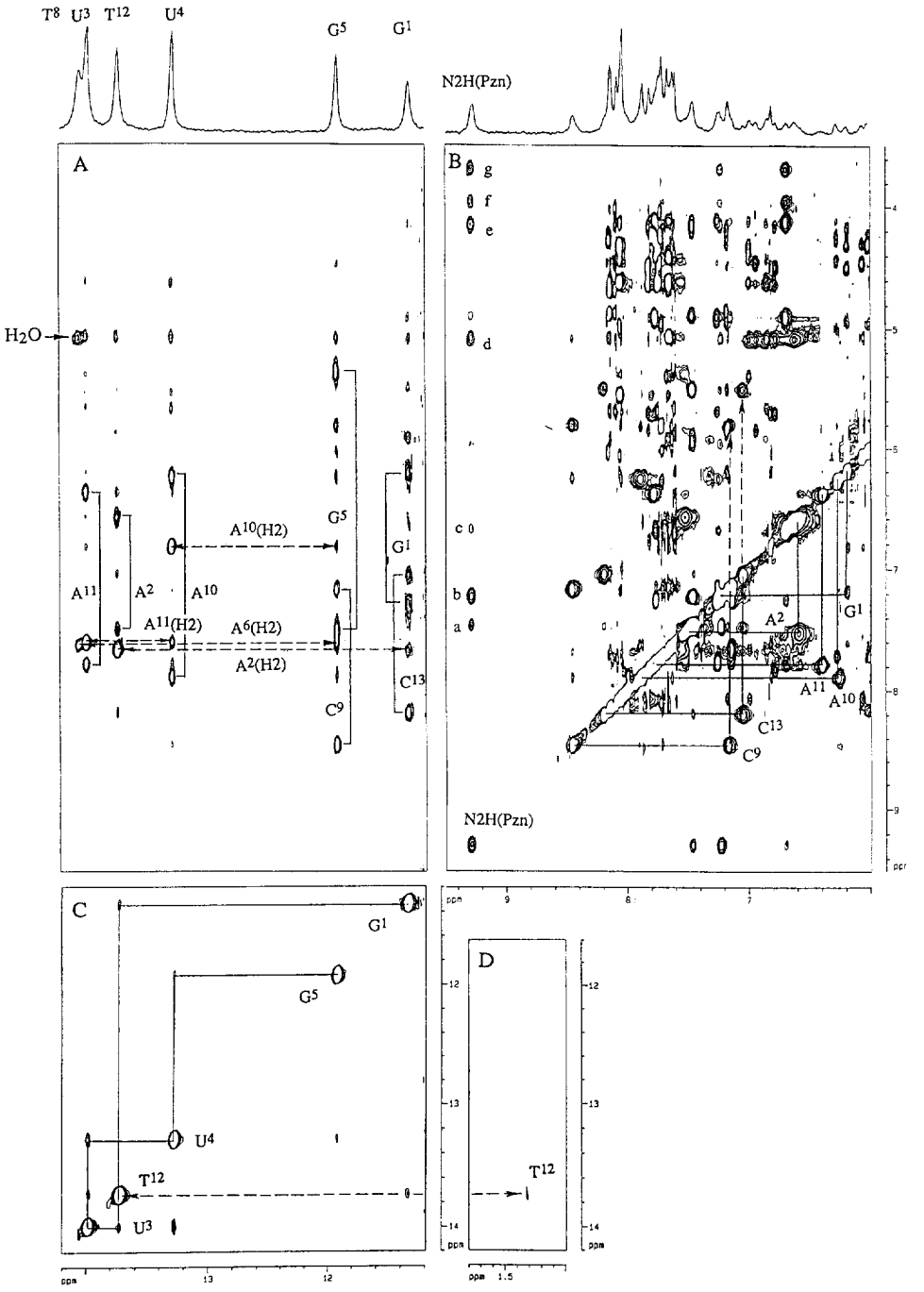
T8 U3 T12 U4 G5 G1
N2H(Pzn)
A
B
C
D
H2O
A10(H2)
A11(H2)
A6(H2)
A2(H2)
A11 A2 A10
G5 G1 C13 C9
N2H(Pzn)
U4
T12
U3
ppm

firstly by the error in the determination of the volume of the cross and diagonal peaks in the NOESY or ROESY spectrum (±20%) [5], secondly, by the standard deviation of the linear regression analyses (90% confidence limit). At the rapid rate of exchange, the decrease of the intensity of the cross and diagonal peaks (or increasing of the linewidth) leads to the increase of the error of determination of the base-pair life-time (τ_o). The activation parameters for the exchange process were obtained from the dependence of the exchange rate (k_{ex}) constants on temperature using the Arrhenius equation: $\ln(k_{ex}) = \ln(A) - E_a/RT$, where E_a is the activation energy and A is the frequency factor. The errors for these parameters are the standard deviation of the linear regression analysis which have been presented with average value of the E_a.

3. Results

3.1. Assignment of the exchangeable protons in the DNA–RNA hybrid duplex

The imino (10–15 ppm) and amino (6–9 ppm) regions of the ^{1}H NMR spectra in H_2O provide information on hydrogen bonding between base-pairs. The spectra of DNA–RNA duplex (I) were recorded at different temperatures to find the optimal condition for making the assignment of all exchangeable protons (Fig. 1A–D) in an unequivocal manner. All imino protons of guanosine, uridine and thymidine residues were assigned (Table 1) by following the connectivity of T(methyl)-T(imino) and imino$_{(i)}$-imino$_{(i+1\ or\ j)}$ (i and j are residue numbers of a next base-paired imino proton from the same or opposite strand) starting at T^{12} methyl proton (Fig. 1A–D). Thus the MeT^{12} (1.34 ppm) ↔ N3HT^{12} (13.73 ppm) crosspeak was linked with both the N3HT^{12} (13.73 ppm) ↔ N1HG^1 (11.33 ppm) and the N3HT^{12} (13.73 ppm) ↔ N3HU^3 (13.99 ppm) crosspeaks (Fig. 1C and D). From the crosspeak of N3HT^{12} (13.73 ppm) ↔ N3HU^3 (13.99 ppm), a connectivity could be

Fig. 1. Expanded plots of the NOESY spectra (200 ms) of the Pzn tethered DNA–RNA hybrid duplex (I) in H_2O/D_2O (90:10%) at 0° C. Crosspeaks in panel (A) show the imino-aromatic/amino proton interactions. The two protons of the amino group of cytosine, adenosine or guanosine are connected by solid line and have been assigned by nucleotide abbreviations (i.e. C, A, G) and its sequence number. The cross peaks between aromatic H2A and imino proton of the nucleobase and its neighbouring (n-1) base-pairs are connected by the dashed lines with the arrow. The row (i.e. at the chemical shift of water in F2 direction) with the crosspeaks between water and imino protons are indicated by symbol (H_2O) with arrow. The assignments of the imino proton resonances are presented in the 1 D spectra on the top part of the panel (A). In the subspectra shown in panel (B) the crosspeaks between amino protons are connected and labled by the solid line. The cross peaks between non-hydrogen bonded NH^b protons (H^a = hydrogen bonded, and H^b = non-hydrogen bonded) and H5 aromatic protons cytosine residues are labeled by dashed lines with arrow. The interactions of imino proton of Pzn linker (N2H) with another protons are labeled as follows with Arabic letters (a–g): aromatic Pzn residue: (a) H4, (b) H3, (c) H1; water: (d); -^{13}CH$_2$-^{14}CH$_2$-Pzn linker: (e), (f) and (g). Subspectra (C) shows the sequential connectivities between imino$_{(i)}$-imino$_{(i+1\ or\ j)}$ (solid line) starting from the connectivity of T(methyl)-T(imino) (dashed line) at T^{12} methyl proton at 1.34 ppm [subspectra (D)].

Table 1
The chemical shifts of the exchangeable imino and amino protons of the $^{5'}$[r(G^{1}A^{2}U^{3}U^{4}G^{5}A^{6}A^7)]$^{3'}$:$^{5'}$p[d(T^{8}C^{9}A^{10}A^{11}T^{12}C^{13})]$^{3'}$Pzn (I) at 0° C

Residue	NH	NH_2 [a]	OH
G^1	11.33	7.28/6.16	6.85
A^2	-	7.50/6.56	6.85
U^3	13.99	-	6.99
U^4	13.28	-	6.77
G^5	11.92	7.20/5.35	6.77
A^6	-	[b]	[b]
A^7	-	[b]	6.93
T^8	14.05	-	-
C^9	-	8.44/7.15	-
A^{10}	-	7.89/6.24	-
A^{11}	-	7.78/6.37	-
T^{12}	13.73	-	-
C^{13}	-	8.19/7.10	-

[a] For NH_2 the first chemical shift is for the hydrogen-bonded proton (H^a) the second for the non-hydrogen-bonded proton (H^b).
[b] Could not be defined.

established to N3HU^3 (13.99 ppm) ↔ N3HU^4 (13.28 ppm) which in turn could be connected with N3HU^4 (13.28 ppm) ↔ N1HG^5 (11.92 ppm) crosspeak (Figs. 1C and D). Finally the N3HU^4 (13.28 ppm) ↔ N1HG^5 (11.92 ppm) could be linked with N1HG^5 (11.92 ppm) ↔ N3HT^8 (14.05 ppm) crosspeak at the end of the double strand (Figs. 1C and D). All amino protons except those of the terminal A^6 and A^7 were assigned using the connectivity rG(imino)-dC(amino^a)-dC(amino^b)-dC(H5)-dC(H6), rG(imino)-rG(amino^a)-rG(amino^b) and dT/rU(imino)-d/rA(amino^a)-d/rA(amino^b) [a and b are the hydrogen-bonded and the non-hydrogen-bonded (more upfield) amino protons, respectively] (Figs. 1A and B). The N1HG^1 (11.33 ppm) imino proton was connected with both N4H^{a}C^{13} (8.19 ppm) and N4H^{b}C^{13} (7.10 ppm), the non-bonded amino proton could in turn be linked to H5C^{13} (5.55 ppm) (Figs. 1A and B). The N1HG^1 (11.33 ppm) imino proton was also connected to N2H^{a}G^1 (7.28 ppm) and N2H^{b}G^1 (6.16 ppm). Such step by step assignments were made for all amino protons (Figs. 1A and B). These assignments were further corroborated using the d/rA(H2$_{(i)}$)-dT/rU(imino$_{(j)}$) (i and j are residue numbers from a complementary base of the opposite strand) and d/rA(H2$_{(i)}$)-(imino$_{(i-1)}$) connectivities. The N1HG^1 (11.33 ppm) imino proton has a crosspeak with H2A^2 (7.68 ppm) which in turn has a crosspeak with N3HT^{12} (13.73 ppm). Similarly, the N3HU^3 (13.99 ppm) ↔ H2A^{11} (7.65 ppm) ↔ N3HU^4 (13.28 ppm), N3HU^4 (13.28 ppm) ↔ H2A^{10} (6.88 ppm) ↔ N1HG^5 (11.92 ppm) and N1HG^5 (11.92 ppm) ↔ H2A^6 (7.71 ppm) ↔ N3HT^8 (14.05 ppm) connections could be established (Fig. 1A) and the H2 protons assigned. The remaining H2 resonance (detected in the inversion recovery experiment) was assigned as H2A^7. Note that the chemical shift of the G^1 imino proton adjacent to Pzn residue is shifted upfield in the same manner as observed earlier in a DNA duplex tethered to Pzn [5].

Table 2

Comparison of the base-pair life-time (τ_{ex}) and the rate of exchange (k_{ex}) of the imino protons of the base pair G^1-C^{13},T^{12}-A^2,U^3-A^{11},U^4-A^{10}, and G^5-(and amino protons of the base pair ^{1}G-^{13}C, and ^{5}G-^{9}C and amino proton of the Pzn tethered DNA–RNA hydrid dupl $^{5'}$[r($G^1A^2U^3U^4G^5A^6A^7$)]$^{3'}$:$^{5'}$p[d($T^8C^9A^{10}A^{11}T^{12}C^{13}$)]$^{3'}$Pzn (I) at different temperatures in the buffer buffer [0.1 M NaCl, 10 mM NaD_2PO_4, 10 mM EDT pH 7.4]

Temp (K)	Imino protons of base pair (^{a} k_{ex} (^{b} τ_{ex}))					Amino protons ^{c} of base-pair (^{a} k_{ex} (^{b} τ_{ex}))				N2H (Pzn)
	G^1-C^{13}	T^{12}-A^2	U^3-A^{11}	U^4-A^{10}	G^5-C^9	C^9H^a	C^9H^b	$C^{13}H^a$	$C^{13}H^b$	
279	5.4 (185)	3.5 (286)	*	3.6 (278)	1.9 (526)	1.3 (763)	1.8 (543)	0.3 (3333)	*	41.0 (24)
281	10.1 (99)	5.0 (200)	*	4.8 (208)	3.3 (303)	2.3 (435)	3.7 (307)	0.4 (2340)	*	53.9 (19)
283	16.3 (61)	10.5 (95)	*	9.1 (110)	5.4 (221)	3.0 (330)	3.5 (286)	1.6 (1584)	*	77.7 (13)
285	24.3 (41)	14.3 (70)	16.0 (62)	16.3 (62)	14.4 (69)	2.5 (398)	4.0 (248)	1.0 (1042)	0.3 (3333)	150.0 (6)
287	35.0 (29)	26.0 (38)	23.0 (43)	26.0 (38)	22.0 (46)	7.9 (127)	10.5 (95)	1.4 (725)	0.5 (2222)	*
289	58.0 (17)	38.0 (26)	39.0 (26)	44.0 (23)	42.0 (24)	20.8 (48)	15.6 (64)	1.9 (510)	0.6 (1818)	*
291	100.0 (10)	58.0 (17)	65.0 (15)	63.0 (16)	54.0 (19)	28.0 (36)	20.0 (50)	2.4 (424)	1.0 (1000)	*
293	200.0 (5)	145.6 (6)	102.0 (9)	159.0 (6)	105.0 (10)	*	*	2.2 (448)	1.3 (775)	*

[a] k_{ex} is the rate of exchange (s^{-1}).

[b] τ_{ex} is the base-pair life time (ms).

[c] H^a = hydrogen bonded, and H^b = non-hydrogen bonded.

The imino proton of the Pzn linker was detectable until 15° C (Fig. 1B). We have subsequently shown, using the MD/MARDIGRAS refinement procedure [6], that this imino proton participates in the hydrogen bonding with the 3′-phosphate group within the linker. The hydroxyl protons of the RNA strand were assigned from their crosspeaks with H1′, H2′ and H3′ of their own sugar (Table 1).

3.2. The rates of exchange of the base-paired imino protons

The rates of exchange (k_{ex}) of the DNA–RNA hybrid duplex (I) at pH 7.4 have been calculated at different temperatures from 6° to 22° C at 2° intervals, and are presented in Table 2. The terminal A^6-T^8 base-pair exchanges rather rapidly and its k_{ex} can not be measured even at 279 K and therefore does not appear in the table. On the other hand, the k_{ex} of G^1-C^{13} base-pair with the Pzn group tethered at the 3′-end of C^{13} is slow and comparable to the k_{ex} of the core base-pairs (A^2-T^{12}, U^3-A^{11}, U^4-A^{10} and G^5-C^9) within the experimental error. The rates of exchange of the imino protons of the AU and AT tracts above 281 K are the same, which are similar to that of the G^5-C^9 base-pair. This means that we are observing the opening-closing process of both the base-pair and the helix [11]. It is noteworthy that the G^1-C^{13} base-pair adjacent to the Pzn residue has only approximately two times higher k_{ex} than the G^5-C^9 base-pair. The two terminal base-pairs G^1-C^{13} and A^6-T^8 show different k_{ex} at all temperatures. They both have additional neighbouring groups (Pzn and an adenosine residue, respectively) which could influence the rate of exchange through stacking interactions. Our previous studies [5] show that Pzn stacks with both base-paired neighbouring bases, and thus reduces the access of the water to the base-paired imino protons. This overall reduction of water availability in turn decreases the k_{ex} of the neighbouring base-pair, G^1-C^{13}, which will be otherwise expected to exchange at a much faster rate for being a terminal base-pair. Similar phenomena has been observed by us earlier in the NMR studies with 5′-Pzn tethered matched DNA duplex [5]. In contrast, the terminal A^7 residue although stacks with its neighbour A^6, as evident [6] by NOE and temperature-dependant chemical shifts, but the k_{ex} of imino proton of the A^6-T^8 base-pair is still very high and can not measured even at a low temperature (279 K). This means that while 3′-Pzn group can efficiently limit the passage of water (hydrophobic effect) through the core retarding the exchange rate of the neighbouring imino protons and thus effectively contributing to the stabilization of the base-pair, the terminal A^7 residue, on the other hand, has no such hydrophobic effect.

The proton exchange life-times (τ_0) of the closed state of the base-pairs in this DNA–RNA duplex (I) were obtained by the extrapolation of the observable life-time (τ_{ex}) of the imino proton versus inverse concentration of the added base catalyst at 6° C (pH 8.4) to infinite concentration (Fig. 2A). We have thus obtained the τ_0 for imino protons for G^1-C^{13}, A^2-T^{12}, U^4-A^{10}, and G^5-C^9 base-pairs, which vary between 0.1–0.8 ms. At 279 K, the imino proton of U^3-A^{11} overlaps with the rapidly exchanging terminal A^6-T^8 base-pair, hence the τ_0 of the former could not be unambiguously estimated. At 285 K, the chemical shift of the terminal A^6-T^8

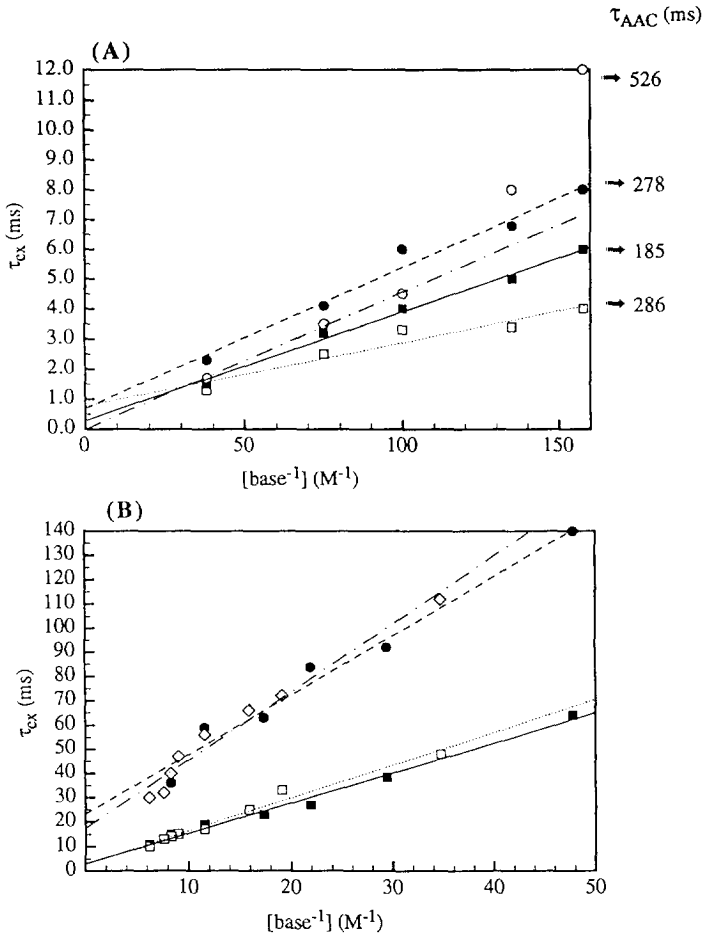

Fig. 2. (A) Ammonia catalysis of the imino proton exchange at 6° C in DNA–RNA hybrid duplex, $^{5'}$[r(GAUUGAA)]$^{3'}$:$^{5'}$p[d(TCAATC)]$^{3'}$-Pzn duplex (I), for the base pairs G^1-C^{13} (■), A^2-T^{12} (□), U^4-A^{10} (●), and G^5-C^9 (○). The life-times at 6° C in the absence of added catalyst (τ_{AAC}) (ms) are presented at the right axis of the plot with arrows. The closed state life-times (τ_o) of the base-pairs have been obtained by extrapolation to the infinite concentration of the base catalyst, which are as follows: 0.3 ± 0.3 ms (G^1-C^{13}), 0.8 ± 0.6 ms (A^2-T^{12}), 0.7 ± 0.7 ms (U^4-A^{10}) and 0.1 ± 0.3 ms (G^5-C^9). (B) A plot of the observed proton exchange life-time (τ_{ex}) versus inverse concentration of ammonia ([base]$^{-1}$ M^{-1}) at 15° C giving the closed-state life-times (τ_o) of the base-pairs for the imino protons of A^{10}-T^{11} (□) and A^9-T^{12} (◇) for the self-complementary 12-mer, $^{5'}$d($C^5G^6C^7G^8A^9A^{10}T^{11}T^{12}C^{13}G^{14}C^{15}G^{16}$)$_2^{3'}$ [duplex (IV)], and for the corresponding imino protons (■) and (●) in the 20-mer, $^{5'}$d($C^1G^2C^3G^4C^5G^6C^7G^8$ $A^9A^{10}T^{11}T^{12}C^{13}G^{14}C^{15}G^{16}C^{17}$ $G^{18}C^{19}G^{20}$)$_2^{3'}$ [duplex (V)]: τ_o for the A^{10}-T^{11} and A^9-T^{12} are 2.9 ± 2.3 ms and 23.2 ± 8.9 ms, respectively, in duplex (V), and τ_o for the corresponding imino protons in duplex (IV) are 2.8 ± 2.2 ms and 17.4 ± 5.4 ms.

imino proton however moved upfield, showing an immeasurably rapid exchange process, which allowed us to estimate the k_{ex} of the imino proton of U^3-A^{11}, which in turn was used to calculate its E_a (see below). It should be noted that the values

of τ_o for all base-pairs are similar (in 0.1 to 0.8 ms range) and much shorter than those obtained for the independent process of opening of AT and GC base-pairs of larger DNA duplexes [10], which range from 20 to 100 ms. To check this phenomena, we have probed the local structure variations by examining the detailed dynamic exchange properties of the imino-protons in three self-complementary DNA duplexes: d[p($^{5'}$p($T^1G^2T^3T^4T^5G^6G^7C^8$)$^{3'}$]:d[$^{5'}$p($C^9C^{10}A^{11}A^{12}A^{13}C^{14}A^{15}$)$^{3'}$] (III), $d(C^5G^6C^7G^8A^9A^{10}T^{11}T^{12}C^{13}G^{14}C^{15}G^{16})_2$ (IV) and $d(C^1G^2C^3G^4C^5G^6C^7G^8A^9A^{10}T^{11}T^{12}C^{13}G^{14}C^{15}G^{16}C^{17}G^{18}C^{19}G^{20})_2$ (V). The comparison of NMR spectral properties amongst the DNA duplexes (IV) and (V) below 21° C (i.e. the proton chemical shifts and the distances between protons estimated from the NOESY spectra of both duplexes [12]) shows that the conformations of duplex (IV) and the 12-mer core (i.e. for ^{5}C to ^{16}G residues) in the 20-mer duplex (V) are very closely similar. An evaluation of τ_{ex} and τ_o under the added ammonia catalysis in a buffered condition [0.150 M NaCl, 0.5 mM NaEDTA with 10 mM ammonia-ammonium chloride buffer at pH 8.8] at the same sample concentration showed that the dynamic behaviour of the imino proton exchange of the core A^9-T^{12} (δ 13.85 ppm) and A^{10}-T^{11} (δ 13.69 ppm) base-pairs of both duplexes (IV) and (V) are quite similar (Fig. 2B). The τ_o for the base-pairs of T^{11} and T^{12} residues in the 12-mer duplex (I) and the 20-mer duplex (IV) at 15° C are as follows: 2.9 ± 2.3 ms and 23.2 ± 8.9 ms in the 20-mer, and 2.8 ± 2.2 ms and 17.4 ± 5.4 ms in the 12-mer, respectively, which are different from the shorter B-DNA duplex (III) that ranges from 0.2 to 4 ms, depending upon the temperature. It is known [10] that the deviation from the B-form of DNA can lead upto 100 times larger τ_o of the A-T tract containing four consecutive A. The present work on our DNA–RNA hybrid and the DNA duplex (III) clearly shows that the A-T(U) tract with three consecutive A has much shorter τ_o than expected [10]. The present data for duplex (I) is also in disagreement with the view [10] that the τ_o of the base-pairs of a DNA duplex increases abnormally as the structure becomes distinctly different from a standard B-DNA: this can be particularly demonstrated from the fact that although the RNA strand is 3′-*endo* and the DNA strand is intermidiary between A- and B-type DNA ($131° < P < 154°$) in the DNA–RNA duplex (I) [6], and yet the τ_o of its base-pairs are much shorter than one would have expected from the literature [10].

In order to obtain the energetic characteristic of the imino proton exchange process with water we have finally plotted the natural log of exchange rates of the imino protons of various base-pairs of the DNA–RNA hybrid duplex (I) and several other short B-DNA duplexes (II) and (III) at pH 7.4 as a function of the inverse temperatures (6 to 22° C at 2° step), which shows a linear dependency (Figs. 3A–E). The slope of the Arrhenius plot thus gives the activation energy (E_a) of the exchange process of imino protons with the bound water [11]. Thus the E_a for the imino protons of the base-pairs in DNA–RNA hybrid duplex (I) are 38.4 ± 3.4 kcal/mol for G^1-C^{13}, 41.4 ± 3.8 kcal/mol for A^2-T^{12}, 42.4 ± 3.0 kcal/mol for U^3-A^{11}, 43.1 ± 3.4 kcal/mol for U^4-A^{10}, 47.1 ± 3.0 kcal/mol for G^5-C^9. The E_a for the imino protons of DNA duplex (II) are 35.6 ± 1.0 kcal/mol (T^3-A^4),

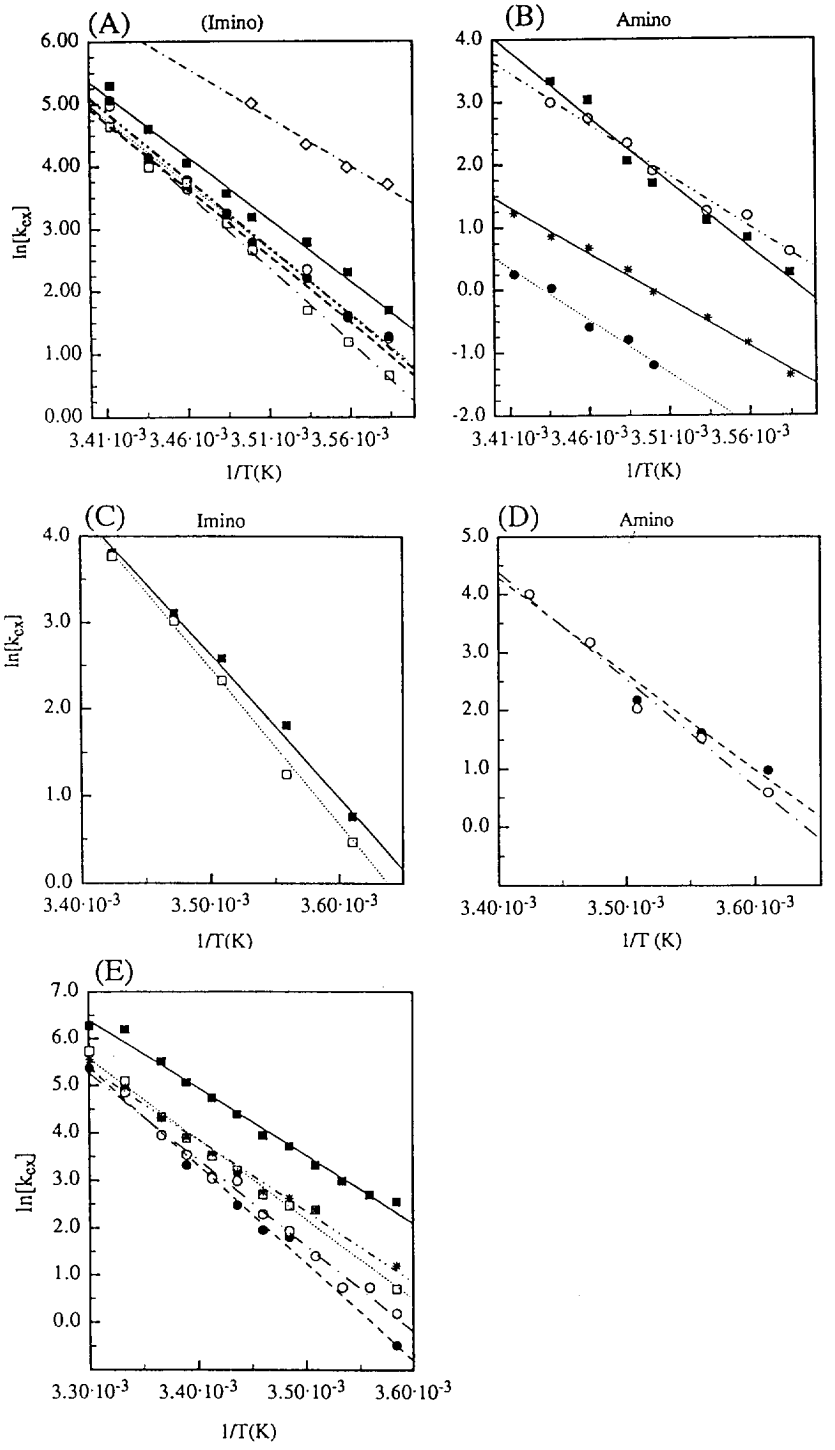
(A)
(Imino)
ln[k_ex]
1/T(K)
(B)
Amino
1/T(K)
(C)
Imino
ln[k_ex]
1/T(K)
(D)
Amino
1/T (K)
(E)
ln[k_ex]
1/T(K)

32.8 ± 2.0 kcal/mol (G^2-C^5). The E_a for the imino protons of DNA duplex (III) are 28.4 ± 1.4 kcal/mol (G^2-C^{14}), 33.6 ± 2.0 kcal/mol (T^3-A^{13}), 40.9 ± 1.9 kcal/mol (T^4-A^{12}), 35.9 ± 2.0 kcal/mol (T^5-A^{11}), and 29.8 ± 0.9 kcal/mol (G^6-C^{10}). The E_a here signifies the total effects from three processes: (i) the base-pair opening-closing rates, (ii) the helix opening-closing rates, and (iii) the exchange of imino protons with water at the open state. The high E_a of the exchange rates of all imino protons in the DNA–RNA duplex (I) as well as in other DNA duplexes (II) and (III) (28-47 kcal/mol) compared to Dickerson's 12-mer DNA duplex (14–15 kcal/mol) [11] suggests that the large activation energy in the smaller duplexes is due to contributions from both the base-pair opening as well as from the helix opening as Tinoco et al originally reported for G-T mismatched 12-mer and 13-mer DNA containing extra adenine [11]. A comparison of E_a of heptameric DNA–RNA duplex (I) with those of the hexameric $d(CGTACG)_2$ (II) suggest that the total picture of the dynamics of the base-pair and the helix opening-closing as well as the exchange rates of imino protons are quite similar and sequence independent despite the fact that the structure of the DNA part of the DNA–RNA hybrid is considerably different from a regular B-DNA duplex [6]. On the other hand, a similar comparison of the E_a at an identical pH of 7.4 of the DNA–RNA hybrid duplex (I), DNA duplex (II) with that of the DNA duplex (III) shows a remarkably different behaviour: the E_a of the core base-pair [40.9 ± 1.9 kcal/mol for T^4-A^{12}] duplex (III) is much larger than the E_a of the base-pairs of the flanking residues. Note however that the E_a of the base-pairs of the flanking residues also decreases step by step as it goes toward the terminal base-pair (from ~ 35 to 28 kcal/mol). This means that the energy penalty for the exchange process of the base-paired imino protons with water at the core part is very high compared to the terminal ones.

When the above data are compared with those of the mismatched analogue of the duplex (III), $d[^5'p(T^1G^2T^3T^4T^5G^6\mathbf{G}^7C^8)^3']:d[^3'(A^{15}C^{14}A^{13}A^{12}\,A^{11}C^{10}\mathbf{A}^9)p^5']$, it is found that all imino protons of the base-pair in G^7-A^{10} mismatched duplex [5] have very similar exchange rates with water at pH 6.4, which are 10–15 fold faster at the core than those of the parent matched duplex (III) at an identical pH. This means that the exchange rates of the imino protons are very sensitive to the number of

Fig. 3. Arrhenius plots for observed k_{ex} (s^{-1}) for $^{5'}$[r(GAUUGAA)]$^{3'}$:$^{5'}$p[d(TCAATC)]$^{3'}$Pzn duplex (I): (A) imino protons [G^1 (■), T^{12} (○), U^3 (∗), U^4 (●), G^5 (□) and Pzn(NH) (◇)], and (B) amino protons [C^9H^a (■), C^9H^b (○), $C^{13}H^a$ (∗), $C^{13}H^b$ (●)]. Similar Arrhenius plots for the B-DNA $d(CGTACG)_2$ duplex (II): (C) imino protons [G^2 (■), T^3 (□)], and (D) amino protons [C^1H^a (●), C^1H^b (○)]. Arrhenius plots for the B-DNA duplex d[p(TDTTTGGC)]:d[p(CCAAACA)] (III): (E) imino protons [G^2 (■), T^3 (□), T^4 (●), T^5 (○), G^6 (∗)]. All k_{ex} have been obtained at pH = 7.4. For NH_2 the label H^a is for the hydrogen-bonded proton and the H^b signifies the non-hydrogen-bonded proton. The activation energies (E_a) (in kcal/mol) are as follows: for duplex (I) imino protons 38.4 ± 3.4 (G^1-C^{13}), 41.4 ± 3.8 (A^2-T^{12}), 42.4 ± 3.0 (U^3-A^{11}), 43.1 ± 3.4 (U^4-A^{10}), 47.1 ± 3.0 (G^5-C^9), amino protons (G^5-C^9) C^9H^a 41.5 ± 4.9 and C^9H^b 32.6 ± 3.3, (G^1-C^{13}) $C^{13}H^a$ 29.4 ± 1.6 and $C^{13}H^b$ 33.2 ± 5.2; for the duplex (II) imino protons 35.6 ± 1.0 (T^3-A^4), 32.8 ± 2.0 (G^2-C^5), amino protons (C^1-G^6) C^1H^a 32.7 ± 4.9 and C^1H^b 36.6 ± 4.9; and for imino protons of duplex (III) 28.4 ± 1.4 (G^2-C^{14}), 33.6 ± 2.0 (T^3-A^{13}), 40.9 ± 1.9 (T^4-A^{12}), 35.9 ± 2.0 (T^5-A^{11}), and 29.8 ± 0.9 (G^6-C^{10}).

nucleotide residues in the oligonucleotide as well as on the sequence and the number mismatches.

3.3. The rates of exchange of the hydrogen-bonded and non-hydrogen bonded amino protons

Because of the smaller size of the duplexes (I) and (II), it has been possible to observe the hydrogen bonded and the non-hydrogen bonded amino protons with two distinctly different chemical shifts. This in turn has made it possible to observe several crosspeaks between the hydrogen bonded and the non-hydrogen bonded amino protons and water and also the separate diagonal peaks for the corresponding amino protons specially for cytosine residues in the NOESY or ROESY spectra from 0° C up to 30° C, which allowed the correct estimation of their volumes as a function of temperature and mixing times. Athough the hydrogen bonded and the non-hydrogen bonded amino protons for some adenine and guanine residues also appeared in the spectra (Fig. 1 and Table 1) but they were not suitable for any calculation because they were either too fast or slow exchanging with water or they were too crowded. The rate of exchange for the hydrogen bonded and the non-hydrogen bonded amino protons of the hybrid DNA–RNA duplex (I) are presented in Table 2. It shows that the rate of exchange of both hydrogen bonded and the non-hydrogen bonded amino protons belonging to C^9 residue are quite similar, whereas the corresponding amino protons of C^{13} residue show a remarkably different behaviour: The similar exchange rates of both hydrogen bonded and non-hydrogen bonded amino protons with water for C^9 residue are due to the fast rotation about its C4 and exocyclic nitrogen bond that takes place in the open state, which is faster than the time scale of the open state of the base-pair (30 to 300 ns) [10]. On the other hand, the rotation around C4 and exocyclic amino group in C^{13} residue is much slower than the time scale of the open state of G^1-C^{13} base-pair, which explains different exchange rates of the two amino protons. The slower exchange rate of the non-hydrogen bonded amino proton of C^{13} residue of G^1-C^{13} base-pair (Table 2) is clearly due to its less acidic pK_a compared to the more acidic hydrogen bonded counterpart, as would be expected from their respective chemical environments. Moreover, it is noteworthy that the exchange rates of amino protons of 3′-Pzn tethered C^{13} are $\sim$2-fold slower than the terminal C^9 located at the other end of the helix, whereas the imino proton of G^1-C^{13} base-pair exchanges at a slightly faster rate than that of G^5-C^9 base-pair (Table 2) at all temperatures studied. These relative exchange rates only exemplifies how the change of the environment could influence the dynamic property of the base-pair. A plot of the natural log of the exchange rates of the both hydrogen bonded and non-hydrogen bonded amino protons of C^9 and C^{13} of the DNA–RNA duplex (I) and the duplex (II) at pH 7.4 as a function of the inverse temperatures (6–22° C, 2° step) shows linear dependency (Figs. 3B and 3D). Thus the slope giving E_a in Fig. 3B and 3D suggest that the exchange rates of amino protons of DNA–RNA hybrid is similar to the B-DNA duplex and is comparable to the exchage dynamics of imino protons.

4. Conclusions

(1) The main difference between B-DNA and DNA–RNA hybrid [6] is that the RNA strand in the DNA–RNA duplex (I) is 3'-*endo* and the DNA strand is an intermediate between A- and B-DNA ($131° < P < 154°$). Secondly, the width of the minor groove for DNA–RNA hybrid is intermediate between the width of the minor grooves in A-RNA and B-DNA form [13]. Thus the intermediary width of the DNA–RNA hydrid duplex uniquely represents a model for studying the dependency of the τ_0 of the imino proton base-pairs on the width of the minor groove. We found that the τ_0 of the DNA–RNA short hybrid duplex (I) is comparable with those of the short B-DNA duplexes (II) and (III). This observation for the first time shows that τ_0 is independant of the width of the minor groove of short duplexes.

(2) The observable E_a consists of at least three different energetic contributions from both base-pair and helix opening-closing as well as from the exchange process of the imino protons from the open state with the bound water. In our studies of DNA–RNA duplex, individual contribution from the above different processes is not separable. What can be however said is that the E_a of the total process operational in DNA–RNA duplex is high and is close to the E_a of the short B-DNA duplex [11].

(3) The E_a of the base-pair and the helix opening-closing as well as from the exchange process of the imino protons are closely comparable to the total observable E_a assessed from the amino protons exchange with the water.

(4) The present investigation emphasizes the need for continued investigation to obtain the energetic characteristic of pH dependent hydration of non-exchangeable protons and correlate those with the thermodynamics of exchange processes of imino and amino protons of the base-pair.

The studies are now in progress with different sizes of oligo-DNA and -RNA to show the length as well as the sequence dependency of the hydration and the exchange process.

Acknowledgements

Authors thank Swedish Board for Technical Development (NUTEK), Swedish Natural Science Research Council (NFR) and Wallenbergstiftelsen for generous financial support. We thank Dr. A.G. Venyaminova, Dr. E.M. Ivanova for their help in the synthesis of Pzn-tethered oligo-DNA–RNA.

References

[1] Thuong, N.T. and Hélène, C., *Angew. Chem.* (Inter. Ed. Engl.), 32 (1993) 666–690.
[2] Gryaznov, S.M. and Lloyd, D.H., *Nucleic. Acid Res.*, 21 (1993) 5909–5915.
[3] (a) Letsinger, R.L. and Schott, M.E., *J. Am. Chem. Soc.*, 103 (1981) 7394–7396. (b) Mergny, J.-L., Boutorine, A.S., Garestier, T., Belloc, F., Rougee, M., Bulychev, N.V., Koshkin, A.A., Bourson, J.,

Lebedev, A.V., Valeur, B., Thuong, N.T. and Hélène, C., *Nucleic. Acid Res.*, 22 (1994) 920–928. (c) Yielding, L.W., Yielding, K.L. and Donoghue, J.E., *Biopolymers.*, 23 (1984) 83–110. (d) Lybrand, T. and Kollman, P., (1985) *Biopolymers.*, 24 (1985) 1863–1879.

[4] (a) Asseline, U., Toulme, F., Thuong, N.T., Delarue, M., Montenay-Garestier, T. and Hélène, C., *The EMBO Journal*, 3 (1984) 795–800. (b) Sun, J.-S., Francois, J.-C., Montenay-Garestier, T., Saison-Behmoaras, T., Roig, V., Thuong, N.T. and Hélène, C., *Proc. Natl. Acad. Sci. USA*, 86 (1989) 9198-9202. (c) Montenay-Garestier, T., Sun, J.S., Chomilier, J., Mergny, J.L., Takasugi, M., Asseline, U., Thuong, N.T., Rougée, M. and Hélène, C. In B. Pullman and J. Jortner (Eds.), *Molecular Basis of Specificity in Nucleic Acid–Drug Interactions,* Kluwer Academic Publisher, Juresalem, 1990, p. 275–291.

[5] (a) Zarytova, V.F., Kutyavin, I.V., Sil'nikov, V.N. and Shishkin, G.V., *Sov. J. Bioorg. Chem.*, 12 (1986) 469–477. (b) Maltseva, T.V., Sandström, A., Ivanova, E.M., Sergeyev, D.S., Zarytova, V.F. and Chattopadhyaya, J. *J. Biochem. Biophys. Methods*, 26 (1993) 173–236. (c) Maltseva, T.V., Agback, P. and Chattopadhyay, J., *Nucleic Acid. Res.*, 21 (1993) 4246–4252. (d) Maltseva, T.V., Yamakage, S.-I., Agback, P. and Chattopadhyaya, J., *Nucleic. Acid. Res.*, 21 (1993) 4288–4295. (f) Bichenkova, E.V., Zarytova, V.F., Ivanova, E.M, Lebedev, A.V, Maltseva, T.V. and Salnikov, G.E., *Bioorgan. Khimi (Russia)*, 18 (1992) 398–412. (g) Bichenkova, E.V, Gorenstein, L.A., Vorob'ev, Yu.N., Tenne, E.Yu., Zarytova, V.F., Ivanova, E.M, Maltseva, T.V. and Lebedev, A.V., *Bioorgan. Khimi (Russia)*, 18 (1992) 901–907.

[6] Maltseva, T.V., Agback, P., Repkova, M.N., Venyaminova, A.G., Ivanova, E.M., Sandström, A., Zarytova, V.F. and Chattopadhyaya, J., *Nucleic. Acid Res.*, 22 (1994) 5590–5599.

[7] (a) Bax, A. and Davis, D.G., *J. Magn. Reson.*, 63 (1985) 207–213. (b) Bax, A., *J. Magn. Reson.*, 77 (1988) 134–147.

[8] (a) Leeflang, B.R., Kroon-Batenburg, L.M.J. and Davis, D.G., *J. Biomolecular NMR*, 2 (1992) 495–518. (b) Farmer II, B.T. and Brown, C.R., *J. Magn. Res*, 72 (1987) 197–202. (c) Griesinger, C. and Ernst, R.R., *J. Magn. Res*, 75 (1987) 261–271.

[9] The AURELIA was supplied by BRUKER.

[10] (a) Guéron, M., Kochoyan, M. and Leroy, J.-L., (1987) *Nature*, 328 (1987) 89–92. (b) Leroy, J.L., Kochoyan, M., Huynh-Dinh, T. and Guéron, M., *J. Mol. Biol.* 200 (1988) 223–238. (c) Leroy, J.-L., Broseta, D. and Guéron, M., *J. Mol. Biol.*, 184 (1985) 165–178. (d) Kochoyan, M., Leroy, J.-L. and Guéron, M., *J. Mol. Biol.*, 196 (1987) 599–609. (e) Leijon, M. and Gräslund, A., *Nucleic. Acid Res.*, 20 (1992) 5339–5343. (f) Fawthrop, S.A., Yang, J.-C. and Fisher, J., *Nucleic Acids Res.*, 21 (1993) 4860–4866. (g) Guéron, M., Charretier, E., Hagerhorst, J., Kochoyan, M., Leroy, J.L. and Moraillon, A., *Structure and Methods, Volume 3: DNA and RNA*, (1990) 113–137.

[11] (a) Pardi, A., Morden, K.M., Patel, D.J. and Tinoco, J.I., *Biochemistry*, 21 (1982) 6567–6574. (b) Pardi, A., Morden, K.M., Patel, D.J. and Tinoco, J.I., *Biochemistry*, 22 (1983) 1107–1113. (c) Pardi, A. and Tinoco, J.I., *Biochemistry*, 21 (1982) 4686–4693.

[12] Yamakage, S.-I., Maltseva, T.V., Nilson, F.P., Földesi, A. and Chattopadhyaya, J., *Nucleic. Acid. Res.*, 21 (1993) 5005–5011.

[13] Fedoroff, O.Yu, Salazar, M. and Reid, B.R., (1993) *J. Mol. Biol.*, 233 (1993) 509–523.